A NOVEL ENGINEERING TOOL FOR THERMAL ANALYSIS OF STRUCTURAL MEMBERS IN NATURAL FIRES

HONG LIANG[1] AND STEPHEN WELCH[2]

ABSTRACT

A novel CFD-based methodology for generalised thermal analysis of protected steel structures in fire has been developed, in order to overcome some of the limitations of detailed thermal analysis methods[1]. Relying on having an appropriate balance of semi-empirical methods and detailed numerical heat transfer approaches, in order to give solutions of sufficient accuracy for structural members in a generalised fashion, the novel methodology has been developed as an essentially 1D heat transfer model[2] with appropriate representations for 2D and 3D effects to reconstruct a quasi-3D solution. The model has been implemented both in spreadsheet format, to facilitate sensitivity studies for model verification and identification of key parameters, and as a submodel within the SOFIE RANS CFD code[3]. Parallel calculations are performed to consider a range of parameters of interest, including member size and protection material properties, as well as uncertainties in some of the essential input parameters (such as emissivities). Model sensitivities are demonstrated, revealing the expected strong dependencies on the properties of the thermal protection materials. Initial validation is undertaken with respect to the full-scale tests on a 12m x 12m compartment at BRE Cardington[4], comparing with the measured temperatures in a protected steel indicative, with satisfactory agreement. Predictions of steel temperatures for variations on the key input parameters will ultimately be provided as field variable predictions by the parallel calculations implemented in the CFD code, thereby providing a much more flexible means of assessing the thermal response of structure to fire than has been available hitherto. The final result is a comprehensive, but practical tool for structural fire design, with potential to improve the efficiency and safety of the relevant constructions.

Keywords: Thermal analysis; CFD; Heat transfer; Numerical modelling; Protected steel

---

[1] PhD student, University of Edinburgh, School of Engineering and Electronics, Edinburgh, UK, email: H.Liang@ed.ac.uk

[2] Lecturer, University of Edinburgh, School of Engineering and Electronics, Edinburgh, UK, email: S.Welch@ed.ac.uk

1. INTRODUCTION

Over the last two decades, attempts to consider more realistically the effects of fire on structures have intensified. This has been motivated in part by the introduction of performance-based codes, which make some provision for design analysis of steel-framed buildings on the basis of the predicted response of structures to "natural" fire exposures. However, in the context of "whole-frame" mechanical analyses, the member temperatures are normally still prescribed very crudely and conservatively, often taking a single worst case temperature value for an entire enclosure. More general methods are required for natural fires, which can better account for localised heating effects.

Simulations based on computational fluid dynamics (CFD) can in principle provide a much more detailed description of the thermal environment and the effects of localised heating. Nevertheless, research to date[1] suggests that detailed thermal analysis of structural members in the context of simulations of full-scale building fires is rather problematic, considering the difference of scale between the mesh which can be afforded for the fire and that required for the thermal analysis of the structure and the high computational demands for coupled analyses. Moreover, with conventional approaches it is necessary to define in advance the specification of the structural members (i.e. section sizes, protection details, thermal properties) and this means that the results may be of very limited application. For example, if on the basis of the simulation results it is decided that any details of the specification need to be modified, or member placement changed, then the whole analysis must be repeated, including the CFD simulation. There is a clear need for much more general and flexible procedures to assess the performance of structures in fire.

In this work a novel methodology is proposed with the aim of creating a more generalised treatment by including computation of a set of "steel temperature field" parameters within the whole of the CFD calculation domain, accommodating, by means of parallel calculations, both uncertainties in the input parameters and possible variants to the specification. By predicting the member temperatures at each point in space the limitations of existing methods with regards to the position of the structural component are bypassed. And by performing parallel calculations which span the range of cases of possible interest, to provide a library of relevant solutions for any given fire scenario, the generality of the results is greatly increased. Considering the potentially great computational costs associated with the large numbers of thermal analysis calculations required (equal to the number of gas-phase cells times the number of variants studied in the parallel calculations), approximate methods are employed to reduce the full 3D thermal response problem down to treatments which are essentially 1D but which include appropriate representations of the heat transfer processes in the other dimensions to reconstruct a quasi-3D solution.

In general the novel methodology relies on having an appropriate balance of semi-empirical methods and detailed numerical heat transfer approaches, tailored to give solutions of sufficient accuracy for problems of interest. A modelling framework which exploits a simple thermal penetration model for the protection[2], coupled to an essentially lumped parameter representation of the steel heating, has been constructed to calculate the thermal response of protected members. Newton-Raphson and Runge-Kutta procedures are used to solve for the surface temperature and to advance the solution in time, respectively, and these treatments have been further developed as submodels within the SOFIE RANS CFD code[3]. The proposed novel methodology has been verified by performing sensitivity studies based on simple spreadsheet implementations and initial validation is reported with reference to the full-scale tests on a 12m x 12m compartment undertaken at BRE Cardington[4].

2. MODELLING PROCESSES

2.1 Problem statement

As aforementioned, the novel methodology is developed through constructing the generalised 1D model and further considering the 2D or 3D effects within the heat transfer processes by appropriate approximations. The computations are performed in each gas-phase CFD cell in the computational domain. The generalised 1D model is constructed through analysing the heat transfer to and within an element in an idealised protected steel member exposed to heat on both faces, as shown in Fig. 1 below:

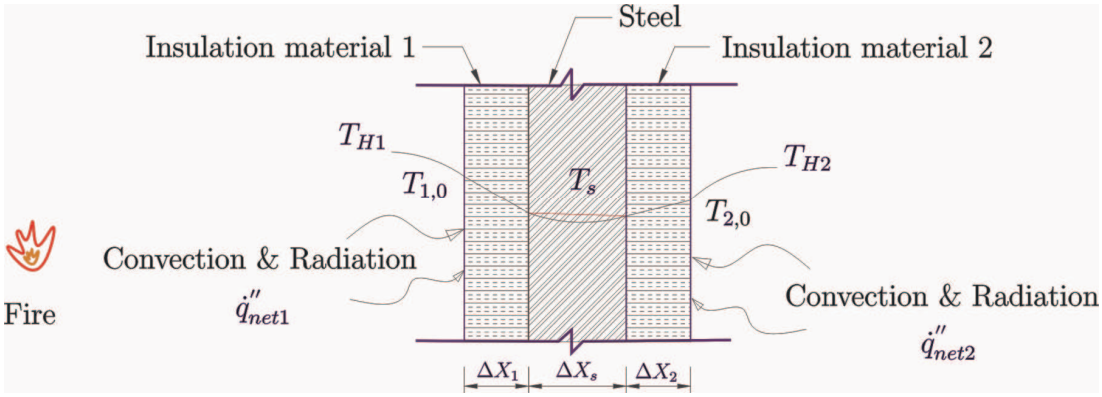

Fig. 1–Temperature distribution from a fire to a protected steel member

This element is supposed to be representative of a slice of a protected steel structure, e.g. a finite section of a flange or a web; two faces are used to allow for situations where the exposure conditions on each side might vary, encompassing also the case of hollow sections with very different exposures on the inside of the structure.

As is well-known in numerical models of heat transfer, the above situation is a strongly coupled problem, with the net heat fluxes at the gas-solid interface very much dependent on the surface temperature, but both also related to the transient thermal response of the structure itself. With simple explicit methods, large numerical errors could arise in the predictions of surface temperature. Therefore, "semi-implicit" methods are adopted here, using Runge Kutta integration to advance each timestep, and strongly link the gas- and solid-phase processes.

A relatively simple treatment has been adopted to implement the generalised 1D model itself, with a lumped parameter model being used for the steel and the coupled thermal response of the protection layer modelled with a semi-empirical treatment for transient heating, allowing for spatially and temporally varying temperature gradients within the solid. The surface temperature, protection material temperatures and the steel temperature are each updated at appropriate time intervals, which might be equal to the CFD timestep, if necessary, but can also be set to longer intervals to improve efficiency (reflecting the fact that the thermal response is normally much slower than evolution of gas-phase conditions).

The implementation of the model takes into account several possible factors which affect the transient response, in particular the temperature-dependent thermal properties, including the effects of moisture in the protection materials. This is important as these properties can have great impact on the thermal response of the structural members, and thus significant errors might occur if only constant values are used[5].

Clearly, for a completely general or comprehensive model, 2 and 3D thermal effects must also be considered. Nevertheless, due to the multiplying computational costs, the novel methodology described here chooses to reduce the full 3D analysis problem into quasi-3D by simply correcting the 1D model results with heat transfer process representations for the other

dimensions, bearing in mind that it is sufficient to determine the "worst" case temperature in the component, and neglecting second-order errors. At present, the following effects are considered:

- Junction effects, i.e. where there is a temperature differential due to the fact that the exposure of one part of the structural component, e.g. a flange or a web, is dominant over that of a connected part;
- End effects, e.g. the cells at the extremity of the flange which are heated from different directions;
- Heat sink effects, e.g. where a beam or column is in contact with ceiling slab;
- Axial temperature gradients, e.g. where a column goes into a hot layer, or where there are significant horizontal temperature gradients.

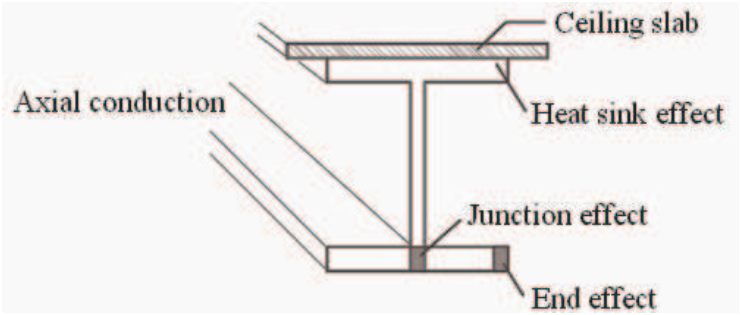

Fig. 2–Cross-section of the beam with locations of possible correction effects

One further complication which arises from the generalised nature of the method is the difficulty in determining means of representing the convective heat transfer to the component when the details of the flowfield over the surface are not specifically computed (as must be the case here). An approximate treatment is proposed, using convention correlations to the local velocities, and in most cases of practical interest radiation will be dominant anyway.

2.2 Conceptual model establishment

2.2.1 Generalised 1D model

Considering the net energy balance with surface heat transfer boundary conditions[2], the 1D model governing equations are derived and given as below:

Energy balance equation:

$$\frac{\partial E_{system}}{\partial t} = \dot{q}''_{net} \tag{1}$$

i.e.
$$\rho_s \cdot c_{ps} \cdot \frac{\partial T_s}{\partial t} \cdot \Delta x_s + w_{p1} \cdot \rho_1 \cdot c_{p1} \cdot \frac{\partial T_1}{\partial t} \cdot \Delta x_1 + w_{p2} \cdot \rho_2 \cdot c_{p2} \cdot \frac{\partial T_2}{\partial t} \cdot \Delta x_2$$
$$= h_{c1} \times (T_{H1}^{(n)} - T_{1,0}^{(n)}) + \dot{q}''_{r1} - \varepsilon_{m1} \cdot \sigma \cdot T_{1,0}^{(n)4} + h_{c2} \times ((T_{H2}^{(n)} - T_{2,0}^{(n)}) + \dot{q}''_{r2} - \varepsilon_{m2} \cdot \sigma \cdot T_{2,0}^{(n)4}$$

The terms shown in the expanded equation here represent, respectively, the transient heating of the steel, the transient heating of each protection layer and convection, radiation and re-radiation for each surface of the protected member. The boundary conditions are supplied from the heat transfer solution for the surfaces, using the following equations:

$$\dot{q}''_{net1} = \frac{k_1}{w_{p1} \Delta x_1} \cdot (T_{1,0}^{(n)} - T_s) \tag{2}$$

i.e. $$h_{c1}\times(T_{H1}^{(n)}-T_{1,0}^{(n)})+\dot{q}''_{r1}-\varepsilon_{m1}\cdot\sigma\cdot T_{1,0}^{(n)4}=\frac{k_1}{w_{p1}\Delta x_1}\cdot(T_{1,0}^{(n)}-T_s)$$

$$\dot{q}''_{net2}=\frac{k_2}{w_{p2}\Delta x_2}\cdot(T_{2,0}^{(n)}-T_s) \qquad (3)$$

i.e. $$h_{c2}\times(T_{H2}^{(n)}-T_{2,0}^{(n)})+\dot{q}''_{r2}-\varepsilon_{m2}\cdot\sigma\cdot T_{2,0}^{(n)4}=\frac{k_2}{w_{p2}\Delta x_2}\cdot(T_{2,0}^{(n)}-T_s)$$

Where:

σ is Stefan-Boltzmann constant, $5.67\times10^{-8}W\cdot m^{-2}\cdot K^{-4}$.

$\dot{q}''_{r1},\dot{q}''_{r2}$ are the incident heat fluxes on each side.

$T_{1,0}^{(n)},T_{2,0}^{(n)}$ represent the surface temperatures between the gas and the solid on each side.

T_s,T_1,T_2 are the steel and average protection layer temperatures, respectively; for the purpose of accounting for the transient energy storage in the protection layer the influence of the change of steel temperature on the protection layer temperatures is included only indirectly, referencing the rate of change on the previous timestep; a more elaborate coupling to the steel temperature change on the current step was investigated, but the effects are small and could not justify the additional computation costs incurred;.

$h_{c1},h_{c2},\varepsilon_{m1},\varepsilon_{m2}$ are the convection parameters and the emissivities of the protection layers.

ρ_s,ρ_1,ρ_2 are the densities of the steel and protection layers, respectively.

$\Delta x_s,\Delta x_1,\Delta x_2$ are the thicknesses of the steel and protection layers, respectively.

w_{p1},w_{p2} are the weight factors of the protection layers, defined in terms of the thermal penetration depth of the protection, more precisely, $w_p=\min\{\frac{A_{actual}}{A_{model}}=\frac{\delta}{\Delta x_p},1\}$ and $\delta=2\cdot\left(\frac{k_p\cdot t}{c_p\cdot\rho}\right)^{1/2}$, the instantaneous thermal penetration depth.

$c_s,c_{p1},c_{p2},k_1,k_2$ are the specific heats of steel and protection layers, and the thermal conductivity parameters, respectively. The temperature-dependent characteristics and moisture effects are incorporated as previously[5]. The effective values are expressed as shown in Figs. 3 and 4, as well as the equations in Tables 1 & 2, below:

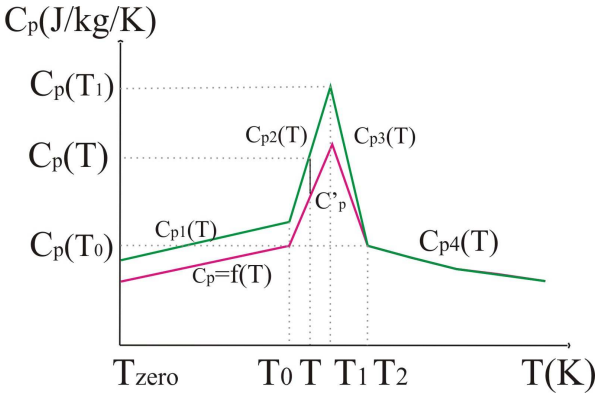

Fig. 3–Specific heat vs. temperature

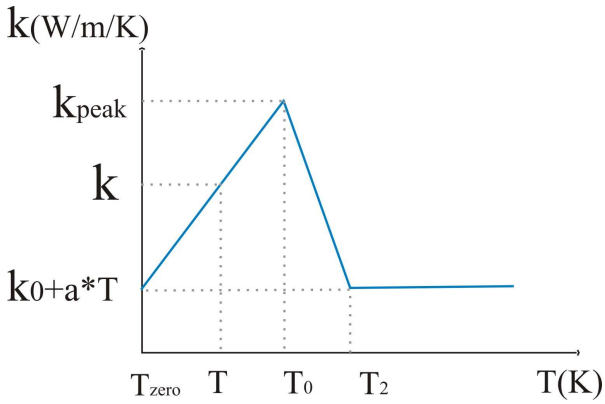

Fig. 4–Thermal conductivity vs. temperature

Table 1: Effective specific heat, c_p

$c_p = c_{p1}(T) = f(T) + c_{p,H_2O} \cdot \omega_m$	$(T_z \le T < T_0)$	(4)
$c_p = c_{p2}(T) = f(T) + c'_{p2}(T) = f(T) + \omega_m \left[\frac{4L}{(T_2 - T_0)} \left(\frac{T - T_0}{T_2 - T_0} \right) + c_{p,H_2O} \left(\frac{T_2 - T}{T_2 - T_0} \right) \right]$	$(T_0 \le T < T_1)$	
$c_p = c_{p3}(T) = f(T) + c'_{p3}(T) = f(T) + \omega_m \cdot \left[\frac{4L}{(T_2 - T_0)} \left(\frac{T_2 - T}{T_2 - T_0} \right) + c_{p,H_2O} \left(\frac{T_2 - T}{T_2 - T_0} \right) \right]$	$(T_1 \le T < T_2)$	
$c_p = c_{p4}(T) = f(T)$	$(T \ge T_2)$	

Table 2: Effective thermal conductivity, k

$k = \left(\frac{T - T_z}{T_0 - T_z} \right) \cdot \left[k_{peak} - (k_0 + a \cdot T) \right] + (k_0 + a \cdot T)$	$(T_z \le T < T_0)$	(5)
$k = \left(\frac{T_2 - T}{T_2 - T_0} \right) \cdot \left[k_{peak} - (k_0 + a \cdot T) \right] + (k_0 + a \cdot T)$	$(T_0 \le T < T_2)$	
$k = k_0 + a \cdot T$	$(T \ge T_2)$	

The solution procedure is based upon using the heat transfer equation boundary conditions (Equs. (2) & (3)) and iterating by the Newton-Raphson method to update the surface temperature, and thereafter, with the updated surface temperatures as boundary conditions, solving the overall energy balance Equ. (1) by the Runge-Kutta method to obtain the steel temperature. During the analysis, while using Newton-Raphson procedures to obtain the values of the surface temperatures, the convergence is checked by the absolute errors $\left| T_{1,0}^{(n)}(i) - T_{1,0}^{(n)}(i-1) \right|$ and $\left| T_{2,0}^{(n)}(i) - T_{2,0}^{(n)}(i-1) \right|$ within each time step, where n represents the time step and i represents the iteration number. By default (in the spreadsheet implementation), five iterations are carried out and reasonably good convergence typically results; in the CFD implementation, iterations are performed until a sufficient degree of convergence is achieved (e.g. 0.1% temperature error). The Runge-Kutta integration is used to accommodate rapid rates of change of gas temperature, to which thermal exposures are related in a strongly non-linear fashion via the radiation terms, and to provide an implicit element to the solution, since the evolving steel temperature is coupled back on itself via its influence on surface temperature. For simplicity, the equations for a 2nd-order Runge-Kutta procedure are provided here, as used in the spreadsheet implementation and initial CFD model, though a 4th-order method will be used in the final CFD implementation. The steel temperature at n^{th} timestep is obtained:

$$T_s^{(n)} = T_s^{(n-1)} + \frac{1}{2}(K_1^{(n)} + K_2^{(n)}) \qquad (6)$$

Where, $K_1^{(n)} = \Delta t \cdot f(T_s^{(n)}, t^{(n)}) = \Delta t \cdot f(T_{1,0}^{(n)}(i_{converged}), T_{2,0}^{(n)}(i_{converged}))$,

While,
$$f(T_{1,0}^{(n)}(i), T_{2,0}^{(n)}(i)) = \left\{ \begin{array}{l} h_{c1} \times (T_{H1}^{(n)} - T_{1,0}^{(n)}(i)) + \dot{q}''_{r1} - \varepsilon_{m1} \cdot \sigma \cdot T_{1,0}^{(n)}(i)^4 \\ + h_{c2} \times (T_{H2}^{(n)} - T_{2,0}^{(n)}(i)) + \dot{q}''_{r2} - \varepsilon_{m2} \cdot \sigma \cdot T_{2,0}^{(n)}(i)^4 \\ - \dfrac{(T_{1,0}^{(n)}(i) - T_{1,0}^{(n-1)}(i))}{\Delta t} \cdot \Delta x_1 \cdot w_{p1} \cdot \rho_1 \cdot c_{p1} \\ - \dfrac{(T_{2,0}^{(n)}(i) - T_{2,0}^{(n-1)}(i))}{\Delta t} \cdot \Delta x_2 \cdot w_{p2} \cdot \rho_2 \cdot c_{p2} \end{array} \right\} \cdot \frac{1}{\Delta x_s \cdot \rho_s \cdot c_{ps}}$$

And, $K_2^{(n)} = \Delta t \cdot f(T_s^{(n)} + K_1^{(n)}, t^{(n)}) = \Delta t \cdot f(\bar{T}_{1,0}^{(n)}(j_{converged}), \bar{T}_{2,0}^{(n)}(j_{converged}))$

While,
$$f(\bar{T}_{1,0}^{(n)}(j), \bar{T}_{2,0}^{(n)}(j)) = \left\{ \begin{array}{l} h_{c1} \times (T_{H1}^{(n)} - \bar{T}_{1,0}^{(n)}(j)) + \dot{q}''_{r1} - \varepsilon_{m1} \cdot \sigma \cdot \bar{T}_{1,0}^{(n)}(j)^4 \\ + h_{c2} \times (T_{H2}^{(n)} - \bar{T}_{2,0}^{(n)}(j)) + \dot{q}''_{r2} - \varepsilon_{m2} \cdot \sigma \cdot \bar{T}_{2,0}^{(n)}(j)^4 \\ - \dfrac{(\bar{T}_{1,0}^{(n)}(j) - \bar{T}_{1,0}^{(n-1)}(j))}{\Delta t} \cdot \Delta x_1 \cdot w_{p1} \cdot \rho_1 \cdot c_{p1} \\ - \dfrac{(\bar{T}_{2,0}^{(n)}(j) - \bar{T}_{2,0}^{(n-1)}(j))}{\Delta t} \cdot \Delta x_2 \cdot w_{p2} \cdot \rho_2 \cdot c_{p2} \end{array} \right\} \cdot \frac{1}{\Delta x_s \cdot \rho_s \cdot c_{ps}}$$

Within these equations, the initial and intermediate surface temperatures, $T_{1,0}^n$ & $T_{2,0}^n$ and $\bar{T}_{1,0}^n$ & $\bar{T}_{2,0}^n$, respectively, are obtained through Newton-Raphson procedures to solve Equs. (2) & (3), in conjunction with the initial steel temperature, in the first case, and the estimated steel temperature between two time steps, $T_s^n = T_s^{n-1} + K_1^{n-1}$, in the second case.

2.2.2 Quasi-3D model

Simple adoption of 1D model for thermal analysis could lead to either conservative (over-design) or non-conservative (unsafe) results. To improve the accuracy in determining the thermal responses of the structural members, a quasi-3D model has been developed which is an essentially 1D analysis, as described above, but including appropriate representations of the heat transfer processes in the omitted coordinate directions. The modelling framework which has been constructed for undertaking these calculations is based on simple physical considerations associated with different possible scenarios. For the time being, four effects are treated for which the precise nature of localised heating is important, as described below:

Junction effects

This correction accounts for the effects of the connection between two different parts of a member under differential heating, e.g. when the main exposure is from below a flange or directly onto the web. In the case where the dominant heating comes from below a flange, for cells in the region of the junction between flange and web, a possible heat sink effect to the cooler structure above the junction needs to be considered. This caters both for the case where the web is cooler, due to having no direct exposure to the dominant radiative heating, and thus some heat would possibly be lost into the web by conduction, and the case where the upper flange of the member is attached to a ceiling slab remaining cool. The effect in depressing the flange temperature can be accommodated in the quasi-3D conceptual model by including an additional term, $-k \times \left(\dfrac{T_s - T_{web}}{\chi} \right)$, on the right-hand side of the 1D model governing equation, Equ. (1), where T_{web} is the independently evaluated web temperature and χ is an appropriate

lengthscale which is a function of the section geometry (section breadth & depth, and flange & web thicknesses). When the dominant heating comes directly on the web, a reverse of the above analysis can be conducted to determine the heat sink into an unexposed flange. It should be noted that in both cases, the effect of the redistribution of heat by conduction serves only to reduce the predicted peak member temperatures, meaning that the initial uncorrected 1D model predictions are expected to be on the conservative side.

End effects

Along the length of the flange, the steel temperature changes, especially for the cells in the two ends of the flange, which might be a worst case position for temperature by virtue of the fact that they are exposed to heat arriving from two different directions, i.e. their heated surface is larger. The heating might be expected to be relatively uniform when convection is dominant and a simple correction referencing the true flange surface area can be used. A more complex case results when the radiative heat flux dominates; if the radiation arrives mainly from below, then the end cell behaves no differently from any other flange cell, or may even be cooler due to the extra surface area for heat loss; if the radiation arrives *only* from the side, then conductive loss to the unexposed material elsewhere in the flange means that the end cell temperature will be depressed, and probably lower than a typical web cell temperature in the same member. At intermediate conditions, the temperature in the end cell, T_s^+, is perturbed and needs carefully consideration; a possible approximate treatment is given below:

$$T_s^+ = T_{s,avg} + \frac{\Delta T_s}{2} \tag{7}$$

Where, $T_{s,avg}$ is the average steel temperature along the flange length, which is equal to the middle point temperature, obtained from the original solution, as per Equ. (6), and ΔT_s is the temperature difference between the flange end-point and the mid-point, by considering the effects of radiation from the side: $\Delta T_s = \frac{b \cdot \dot{q}_{rad,side}}{k}$, where b is flange width.

Heat sink effects

This case considers the thermal effects when a structural member is in contact with a ceiling slab. Here, the upper flange in the model is assumed to be cooler than the rest of the member, and can be ignored. For the lower flange, heat sink effects may lead to an overly-conservative solution and a correction might be justified. The solution, together with the correction for this case, is similar to that for junction effects described above.

Axial temperature gradients

When the structure passes from a cold layer into a hot layer, i.e. a column or even in very deep section beams, the temperature changes greatly with height. The former could introduce significant modelling errors but the latter is normally likely to be less significant in terms of peak temperatures and thus is neglected here. It is however important to note that any resulting modelling errors will be on the conservative side. This can be explained by the fact that the temperatures of cells in the hot layer are reduced by axial conduction to the cooler structure below, whilst the temperatures of the cooler cells are increased - but still remain *below* those of the structure where it is exposed to the highest temperatures. The governing equation for analysis of a single cell at an intermediate height in a column running through a thermal stratified layer is:

$$\begin{aligned} &h_{c1} \times (T_{H1} - T_{1,0}{}^{(n)}) + \dot{q}''_{r1} - \varepsilon_{m1} \cdot \sigma \cdot T_{1,0}{}^{(n)4} + h_{c2} \times (T_{H2} - T_{2,0}{}^{(n)}) \\ &+ \dot{q}''_{r2} - \varepsilon_{m2} \cdot \sigma \cdot T_{2,0}{}^{(n)4} + \frac{k}{\delta_{x,upper}} \cdot (T_{s,upper} - T_s) - \frac{k}{\delta_{x,lower}} \cdot (T_s - T_{s,lower}) = 0 \end{aligned} \tag{8}$$

Compared with 1D model governing equations, two additional correction terms $\frac{k}{\delta_{x,upper}} \cdot (T_{s,upper} - T_s)$ and $\frac{k}{\delta_{x,lower}} \cdot (T_s - T_{s,lower})$ appear, due to the heat conduction effects, where *upper* is a characteristic hot layer temperature and *lower* signifies conditions in a cold(er) layer. The significance of the correction terms depends on the location of the element in question with respect to the bounding temperatures, and they cancel for an element midway between hot and cold positions in an assumed linear temperature gradient region. Note that the model provides an approximate treatment, with $T_{s,upper}$ and $T_{s,lower}$ typically being defined at the two remote locations, thereby representing peak gradients; no attempt is made to take into account the more detailed temperature profile over the height of the column, in order to avoid the additional computational expense of performing the necessary calculations.

2.3 Verification and validation of the models

The above conceptual models are firstly implemented in a spreadsheet-based model. Representative empirical values are adopted for some terms such as the initial conditions, the dry thermal properties, moisture content, etc., and their influence has been studied by exercising the model with different sets of input parameter values. The conceptual models are also implemented into SOFIE CFD code[3].

The performance of the model was assessed by performing sensitivity studies, looking at the effects of a range of numerical and physical parameters. Comparisons were also made with the results of a simplified version of the model, labelled "simplified method", which advances the solution using an explicit one-step scheme, i.e. bypassing the Runge-Kutta integration used in the main method. To provide a further comparison, the simple empirical model for protected members described in Eurocode 1 is also implemented.

The test case used for verification studies is the protected steel indicative, UC254x254/73, in the full-scale tests on a 12m x 12m compartment undertaken at BRE Cardington[4]; this member was protected with about 25mm of Fendolite MII sprayed fibre (ρ=680kg/m^3, k=0.19W/m/K). In the test a variety of thermal parameter measurements were made, encompassing conditions in the gas phase (temperatures, velocities and heat fluxes) and in the solid phase (steel temperatures in protected beams, columns and indicatives with and without protection)[5]; this study also serves for an initial validation of the model, comparing the model predictions with the measured steel temperatures in the protected indicative.

3. PRELIMINARY RESULTS AND DISCUSSION

3.1 Simulation results

Fig. 5 shows the results of the spreadsheet-based generalised 1D model simulation. These are obtained by using the same protection materials on each side of the steel, protection thickness: $\Delta x_1 = \Delta x_2 = 25mm$ and steel flange thickness: $\Delta x_s = 14.2mm$, with moisture content 1%, fire emissivity 0.8, member emissivity 0.9 and h_c = 8W/m^2/K[1]. The results are reasonable and in-line with expectations.

Fig. 6 shows a comparison of the predictions of steel temperature with the test. There is a reasonable agreement though some differences are apparent. The "novel" method results differ significantly from the "simplified" method, thereby justifying the effort made to introduce full coupling; the predictions of Eurocode 1 initially lie between those of the new models, but eventually exceed the measure temperatures (a conservative result); a more precise match with the test results is easily achieved by adopting a temperature dependent conductivity, with a very slight negative temperature correlation.

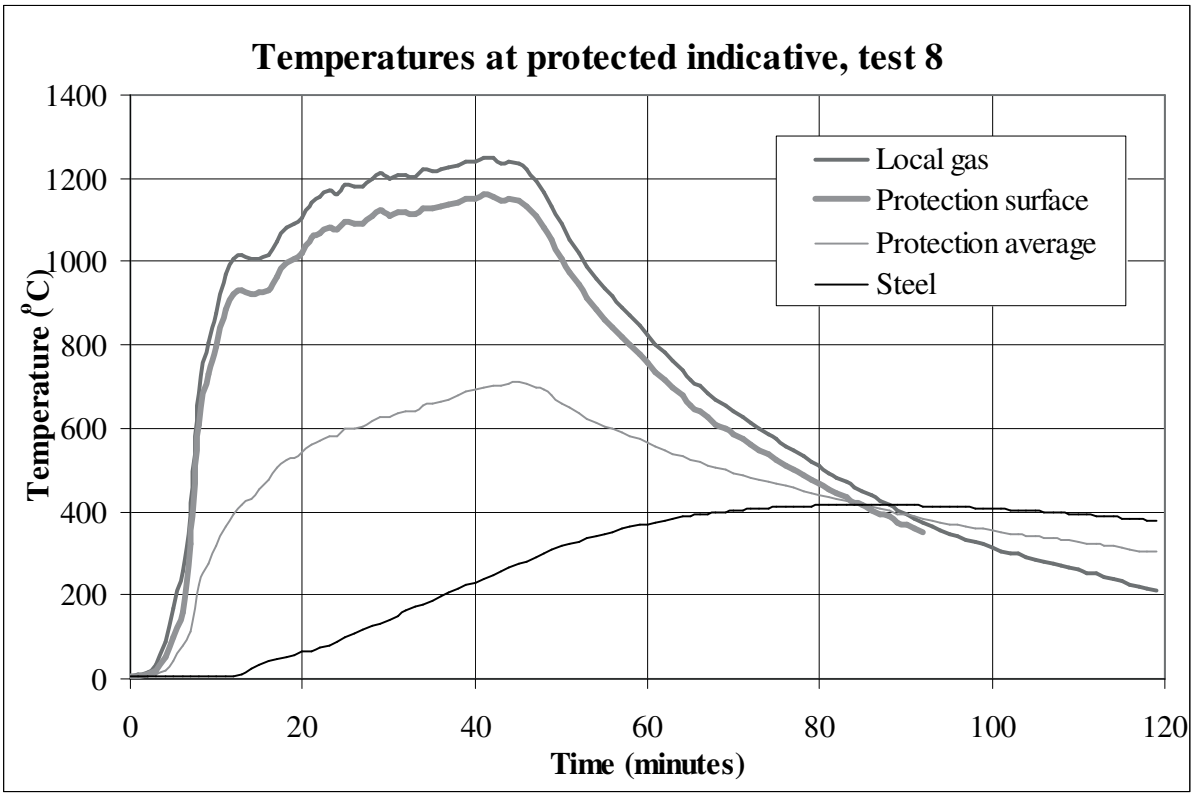

Fig. 5 –Temperature change with time using improved method

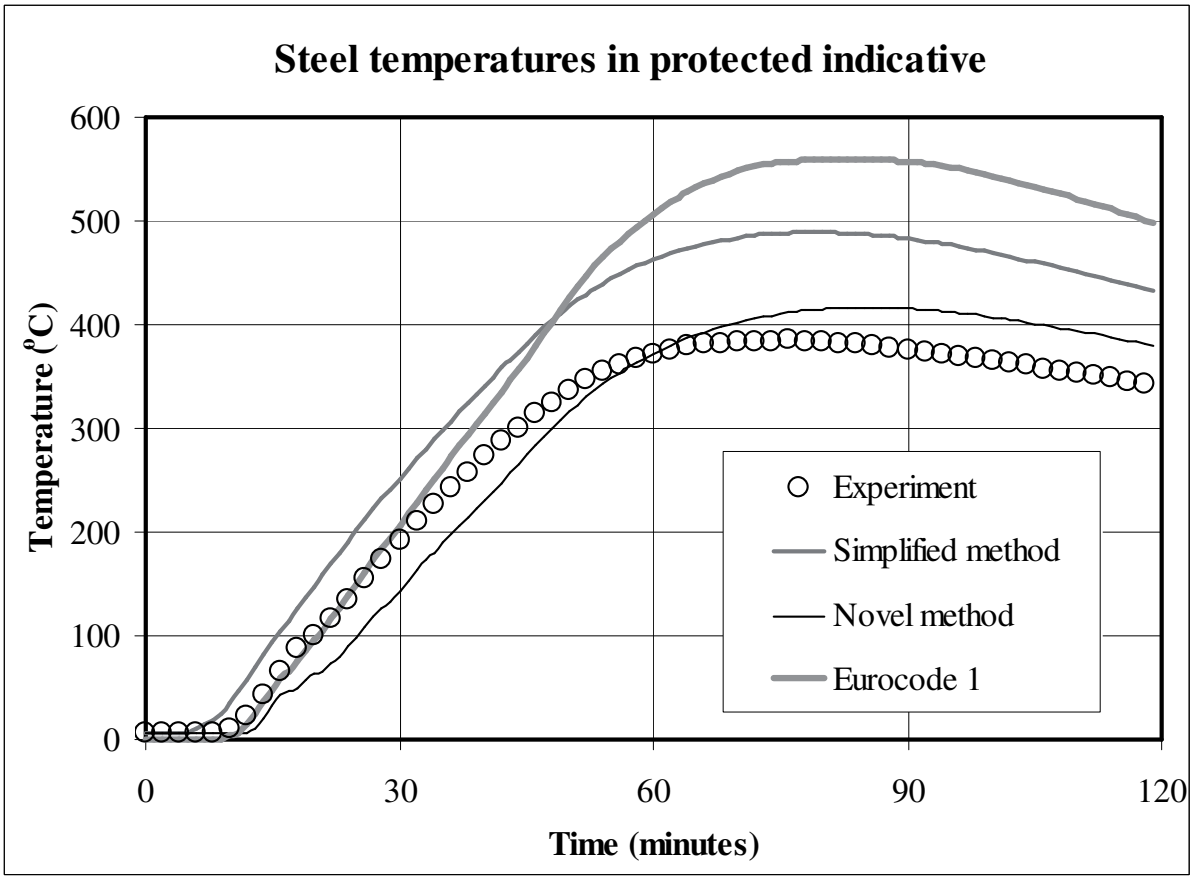

Fig. 6–Comparison of steel temperature change with time using different methods

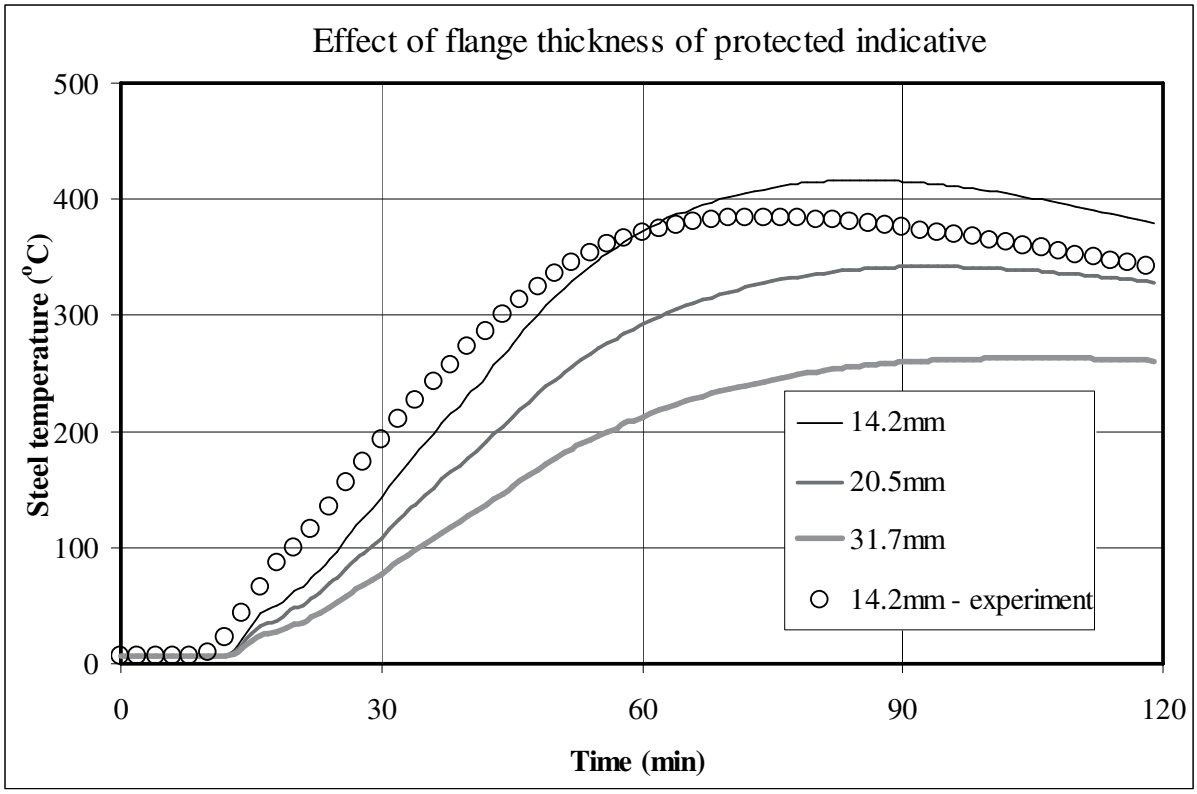

Fig. 7–Effect of flange thickness on steel temperature

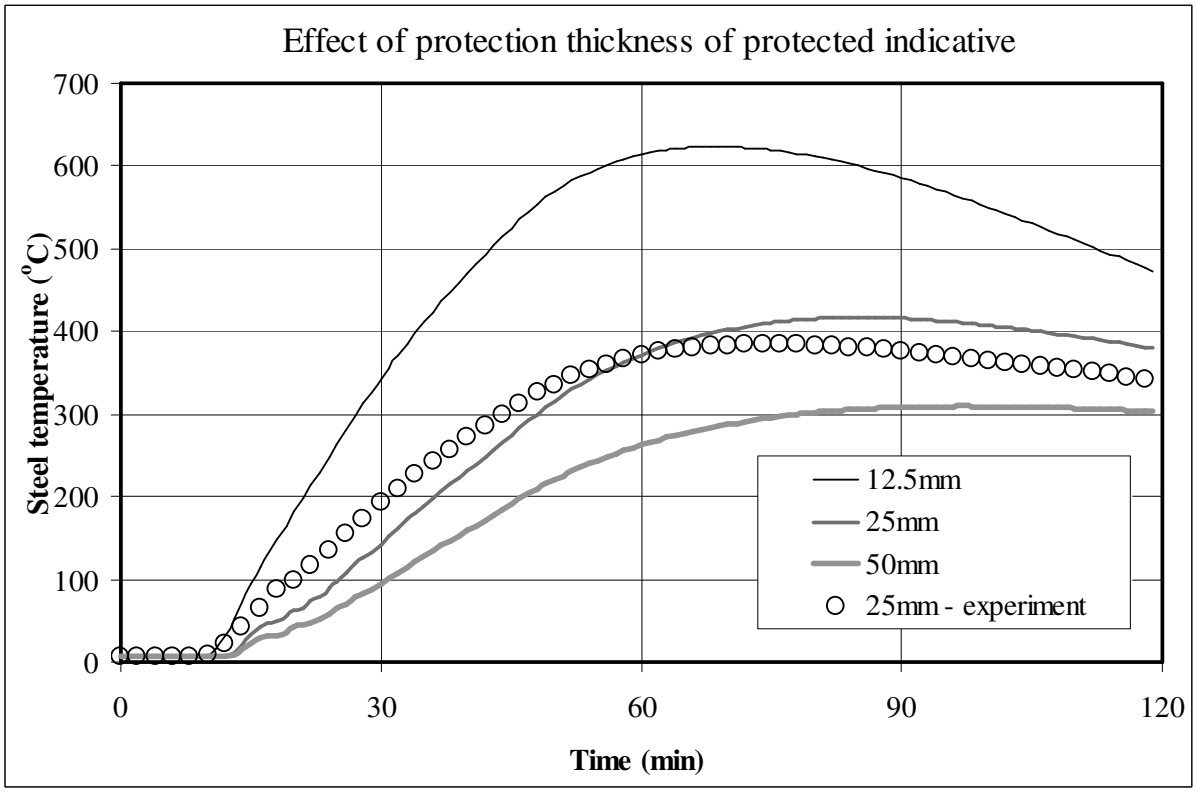

Fig. 8–Effect of protection thicknesses on steel temperature

3.2 **Sensitivity study results**

A couple of results from the sensitivity study are shown in Figs. 7 and 8 for the effects of changing the steel flange thickness (spanning UC 254x254/73,107,167) and the protection thickness (12.5 to 50mm). The results for changing the protection thermal conductivity mirror the latter, and show the expected strong influence of protection properties. This is the type of information which will be provided by the CFD implementation of the method.

4 CONCLUSIONS

A novel CFD-based methodology for generalised thermal analysis of protected steel structures in fire is described. The method is based on a 1D heat transfer analysis, but appropriate corrections are developed to reconstruct a quasi-3D solution. The new 1D model has been implemented both in spreadsheet format, permitting sensitivity studies for verification, and as a submodel in the CFD code. Initial results confirm the sufficiency of the algorithms adopted, and indicate some of the model sensitivities, with strong dependencies on the properties of the thermal protection materials. Comparisons with the measured temperatures in a steel indicative located in a post-flashover fire in a full-scale fire test show a sufficient agreement. Predictions of steel temperatures for variations on member and protections specifications will ultimately be provided as field variable predictions by the parallel calculations implemented in the CFD code, thereby providing a much more flexible means of assessing the thermal response of structure to fire than has been available hitherto.

5 ACKNOWLEDGEMENTS

The authors gratefully acknowledge the financial support from BRE Trust and technical supports from both BRE fire research group and the other members of the BRE Centre for Fire Safety Engineering at the University of Edinburgh.

6 REFERENCES

[1] Kumar, S., Welch, S., Miles, S. D., Cajot, L.-G., Haller, M., Ojanguren, M., Barco, J., Hostikka, S., Max, U. & Röhrle, A., "Natural Fire Safety Concept - The development and validation of a CFD-based engineering methodology for evaluating thermal action on steel and composite structures", European Commission Report EUR 21444 EN, 150 pp., ISBN 92-894-9594-4, 2005.

[2] Carslaw, H.S. & Jaeger, J.C. “Conduction of Heat in Solids”, Oxford University, 1959.

[3] Lewis, M.J., Moss, J.B. & Rubini, P.A., "CFD modelling of combustion and heat transfer in compartment fires", in Proc. 5th Int. Symp. on Fire Safety Science, pp. 463-474, 1997.

[4] Lennon, T. & Moore, D., “The natural fire safety concept—full-scale tests at Cardington”, Fire Safety Journal, vol 38, no. 7, pp. 623-643, 2003.

[5] Welch, S., "Developing a model for thermal performance of masonry exposed to fire", 1st International Workshop on "Structures in Fire", Copenhagen, June 2000.

[6] British Standard Institute. Eurocode 1: *Actions on structures – Part 1-2: General actions – Actions on structures exposed to fire.* CEN 2002.

[7] British Standard Institute. Eurocode 3: *Design of steel structures – Part 1-2: General rules – Structure fire design.* CEN 2002.